FREQUENCY DEPENDENCE OF SEISMIC DATA FROM NIGERIA: PRELIMINARY RESULTS

Mary L. Krasovec, Daniel R. Burns, and M. Nafi Toksöz

Earth Resources Laboratory
Department of Earth, Atmospheric, and Planetary Sciences
Massachusetts Institute of Technology
Cambridge, MA 02139

ABSTRACT

Seismic data from the Niger Delta is used to test processing sequences involved in prestack and poststack amplitude and frequency analysis of marine seismic data. Water bottom reverberations are found to present a formidable challenge in poststack frequency and amplitude analysis. However, reflectors with anomalously high amplitudes show low frequency content both in deconvolved poststack data and in the near offsets of prestack data with no deconvolution, which agrees with results in the literature. Lack of detailed knowledge of the lithology prevents investigation of the physical nature of the amplitude and frequency variations.

INTRODUCTION

Recent research suggests the usefulness of frequency content analysis of seismic data. For example, Eastwood *et al.* (1994) found a correlation between the attenuation of high frequencies and the presence of gas in a shallow bitumen reservoir undergoing steam injection. Schmitt (1998) found instantaneous frequencies to be 20–30 Hertz lower near well bores during steam injection, coinciding with anomalously high reflection amplitudes. Radovich and Oliveros (1998) use instantaneous amplitudes and frequencies to map deep sand channels, finding high amplitudes and low frequencies in the clean, coarse sands. In this case, the low frequency content is attributed to the geometry of the sands. Shen (1998) finds correlation between the presence of fractures and the scattering of high frequencies and uses frequency variation with offset (FVO) and azimuth to map fracture set orientations.

We note that frequency dependence, like amplitude variation with offset (AVO), can have many different lithological and geometrical causes and is difficult to interpret.

To date there are relatively few detailed theoretical studies of the rock physics behind frequency variation. This paper is part of an ongoing project to quantify the causes of frequency variation.

SEISMIC DATA

Our data is from the Niger Delta off the west coast of Africa. Producing fields in the area are characterized by marine shales with local sandy and silty beds thought to have been laid down as turbidites and continental slope channel fills (Ibie, 1997). The structure of the Niger Delta is predominantly characterized by listric faults with associated rollover anticlines. The facies consist of interbedded high-energy deltaic sandstones, siltstones and shales, and the region is known to have large reserves of natural gas.

A stacked section of our data set (Figure 1) shows some of the features mentioned above. Since well log data has not been released, this data set is being used only as a test of the processing sequence and frequency calculations. Our knowledge of the regional geology does allow a basic interpretation of the section: We see listric normal faults trending upper left to lower right, and we interpret the shallow bright reflector at CDPs 220 through 270 and two-way time 0.6 seconds, to be a gas reservoir. The bright spot at CDP 300 to 350 and two-way time 1.5 seconds could also be a hydrocarbon reservoir. Figure 1 shows four reflectors of interest; the shallowest two, reflectors 1 and 2, pass above and through the shallow bright spot. Reflectors 3 and 4 are deeper horizons that appear to terminate at the fault. Reflector 3 shows an increase in amplitude near the fault, suggesting an accumulation of hydrocarbons sealed by the fault. We will concentrate on these reflectors in our analysis, with reflectors 1 and 4 assumed to be background, and the brighter parts of reflectors 2 and 3 being anomalies.

Our processing sequence attempts to preserve the amplitude and spectrum of the data as much as possible. We use spherical divergence amplitude corrections and apply an FK filter to minimize the water bottom reverberations. Figure 2a shows the shot gather with only gain corrections and a band pass filter to remove low frequency noise, Figure 2b shows the same shot gather after FK filtering. To pick the horizons of interest, we apply deconvolution and do a velocity analysis, then stack the data as shown in Figure 1. From the stack we choose the zero offset times and stacking velocities of the events of interest. We use these to define a moveout curve in the prestack domain (with no deconvolution), such as the solid line shown for synthetic data in Figure 3. A window of constant width is taken at each offset, shown as dashed lines. The traces in each window are then analyzed for amplitude and frequency content, shown in Figure 4.

We use two methods of frequency analysis: Instantaneous properties derived from complex trace analysis (Taner *et al.,* 1979) and the multiple signal classification (MUSIC) method (Schmidt, 1986), which is useful for power spectrum estimation of short traces (Shen, 1998).

Following the method of Shen (1998) we describe the frequency dependence of the poststack data by doing a linear least square fit of peak frequency versus offset, re-

sulting in values for FVO slope and FVO intercept at each point along the poststack reflector. Similarly, for the amplitude variation, we estimate the incidence angle θ for each poststack trace and find AVO slope and AVO intercept from a plot of amplitude versus $\sin^2\theta$.

RESULTS

Figures 5 and 6 are the frequency and amplitude analysis results for two CMP locations along horizon 3, at about 1,550 ms. Figure 5 is taken at CMP 315, where the stack shows a bright spot. Figure 6 is at CMP 425 further along the horizon, where the reflection is not so bright.

We note that the plot of frequency versus offset has a great deal of scatter. In fact, no clear correlation between peak frequency and offset is found conclusively. This is obvious from the lack of coherent peaks in the traces, shown in the top subplot.

The amplitude versus angle plot shows similar problems. We note the sudden changes in amplitude at middle offsets, part of which we attribute to an artifact of the FK filtering of the linear arrivals. Figures 2a and 2b show the unevenness of reflectors amplitudes in shot gathers, with and without FK filtering.

Figure 7 shows the FVO slope for the four horizons. We see that the values are all extremely small and show no correlation with the bright amplitude regions. On the other hand, the FVO intercept shown in Figure 8 shows low frequencies in the regions with bright reflections.

Figure 9 shows the instantaneous frequency for the four horizons of interest in the deconvolved poststack data. The bright reflectors show low frequencies in agreement with the poststack FVO intercepts shown in Figure 8.

CONCLUSIONS

Preliminary results show, both in the poststack domain and at near offsets, a correlation between low frequency content and large amplitude reflections in areas thought to contain hydrocarbon reservoirs. However, linear arrivals in the raw data due to direct waves and water bottom reverberations severely limit our ability to analyze the data in the prestack domain. Future processing schemes need to address this issue.

ACKNOWLEDGMENTS

This work was supported by the Borehole Acoustics and Logging/Reservoir Delineation Consortia at the Massachusetts Institute of Technology.

REFERENCES

Eastwood, J., Lebel, P., Dilay, A., and Blakeslee, S., 1994, Seismic monitoring of steam-based recovery of bitumen, *The Leading Edge, 13,* 242–251.

Ibie, E., 1997, Seismic stratigraphic analysis in the Niger Delta: A case study of the Benin River 3-D seismic cube, M.S. thesis, Massachusetts Institute of Technology.

Radovich, B.J., and R.B. Oliveros, 1998, 3-D sequence interpretation of seismic instantaneous attributes from the Gorgan field, *The Leading Edge, 17,* 1286–1293.

Schmidt, R., 1986, Multiple emitter location and signal parameter estimation, *IEEE Transaction on Antennas and Propagation, AP-34,* 276–280.

Schmitt, D.R., 1998, Seismic Attributes for monitoring of a shallow heated heavy oil reservoir: A case study, *Geophysics, 63,* 368–377.

Shen, F., 1998, Seismic characterization of fractured reservoirs (Part I); Crustal deformation in the Tibetan plateau (Part II), Ph.D. thesis, Massachusetts Institute of Technology.

Taner, M.T., Koehler, F., and Sheriff, R.E., 1979, Complex seismic trace analysis, *Geophysics, 44,* 1041–1063.

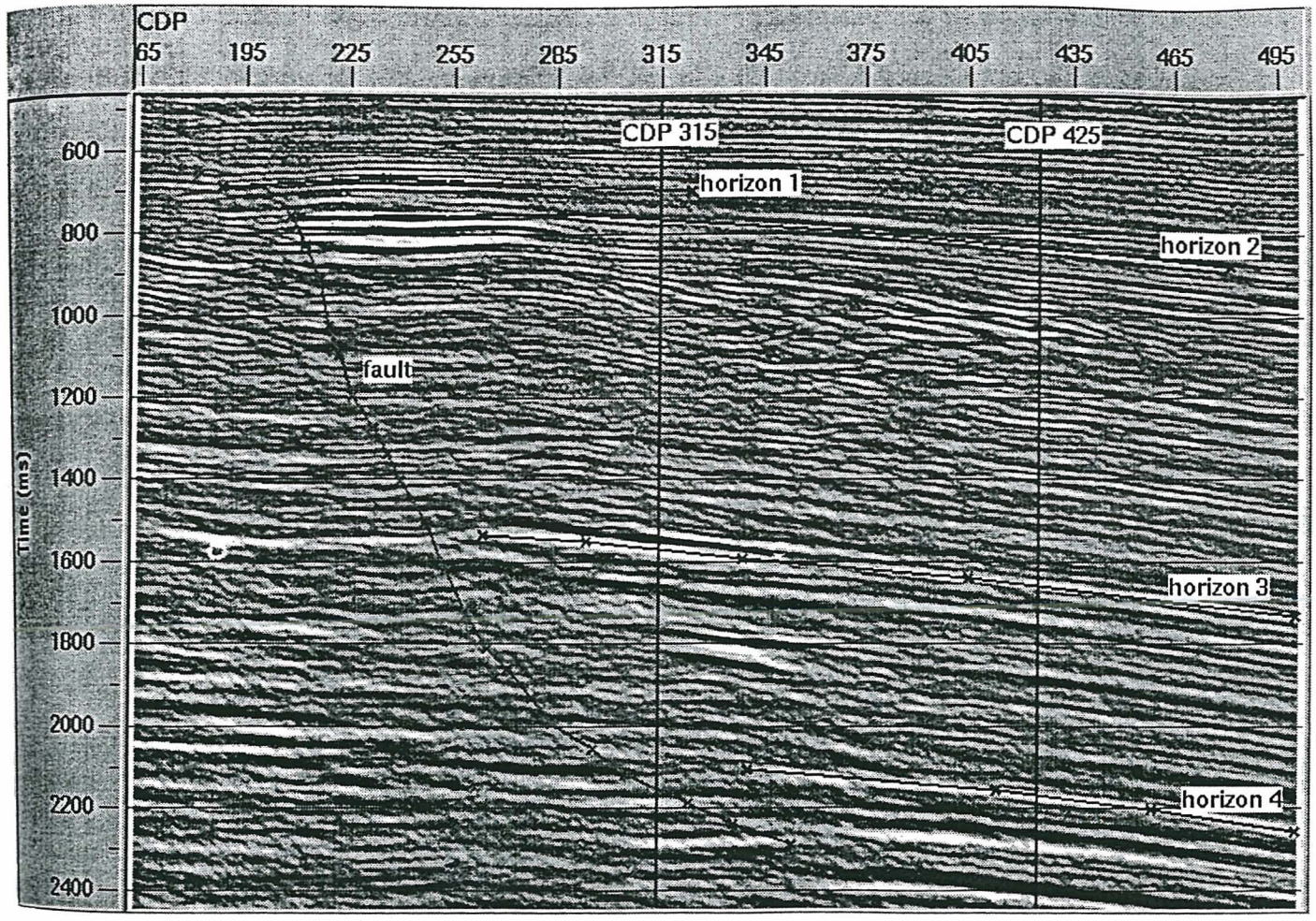

Figure 1: The stacked section with a possible fault location and horizons of interest marked. Horizons 1 and 2 pass above and through the shallow bright spot. Reflectors 3 and 4 are deeper horizons that appear to terminate near the fault.

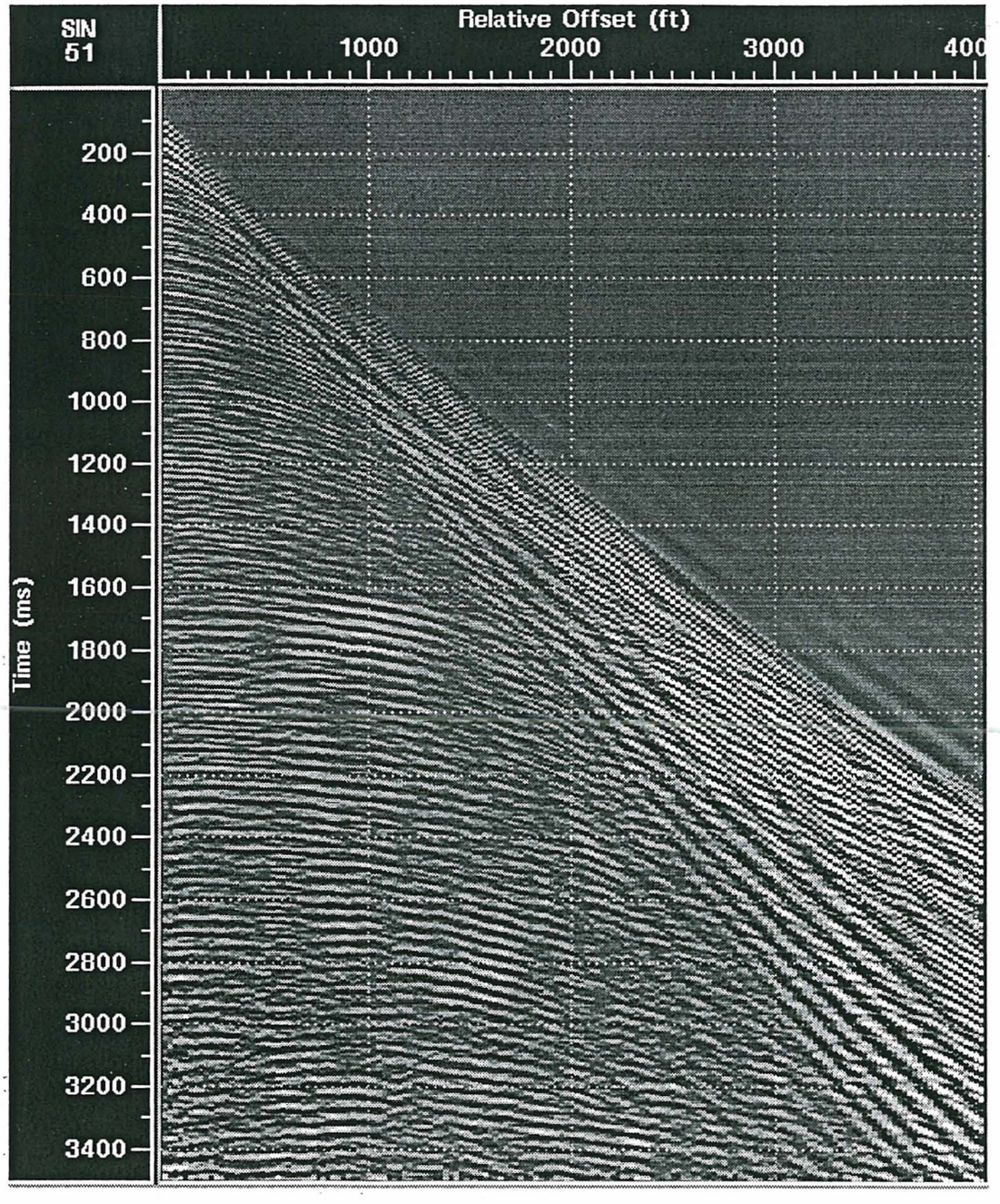

Figure 2a: A shot gather with spherical divergence amplitude correction and bandpass for low frequency noise.

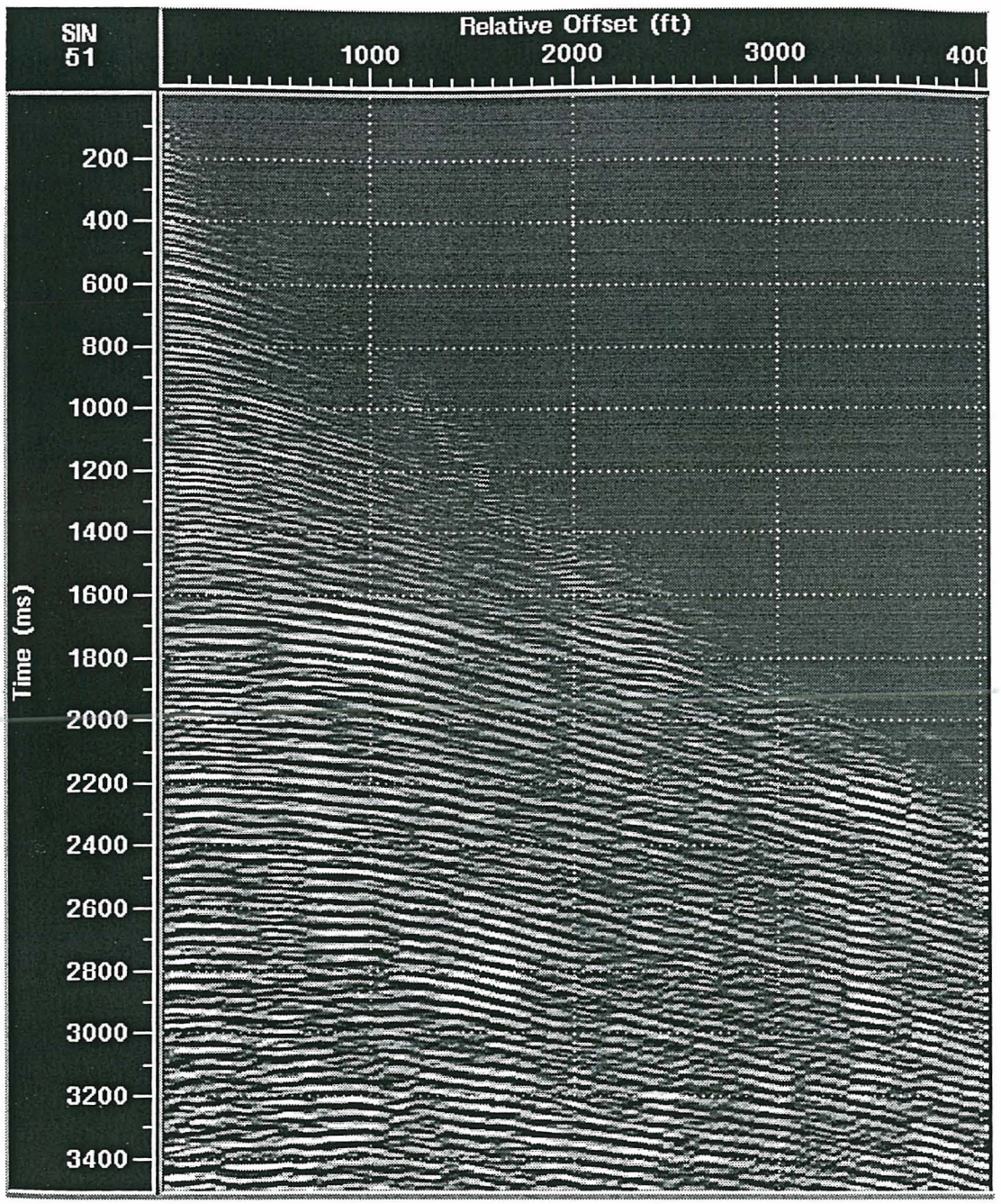

Figure 2b: The same shot gather as in Figure 2a with FK filtering applied.

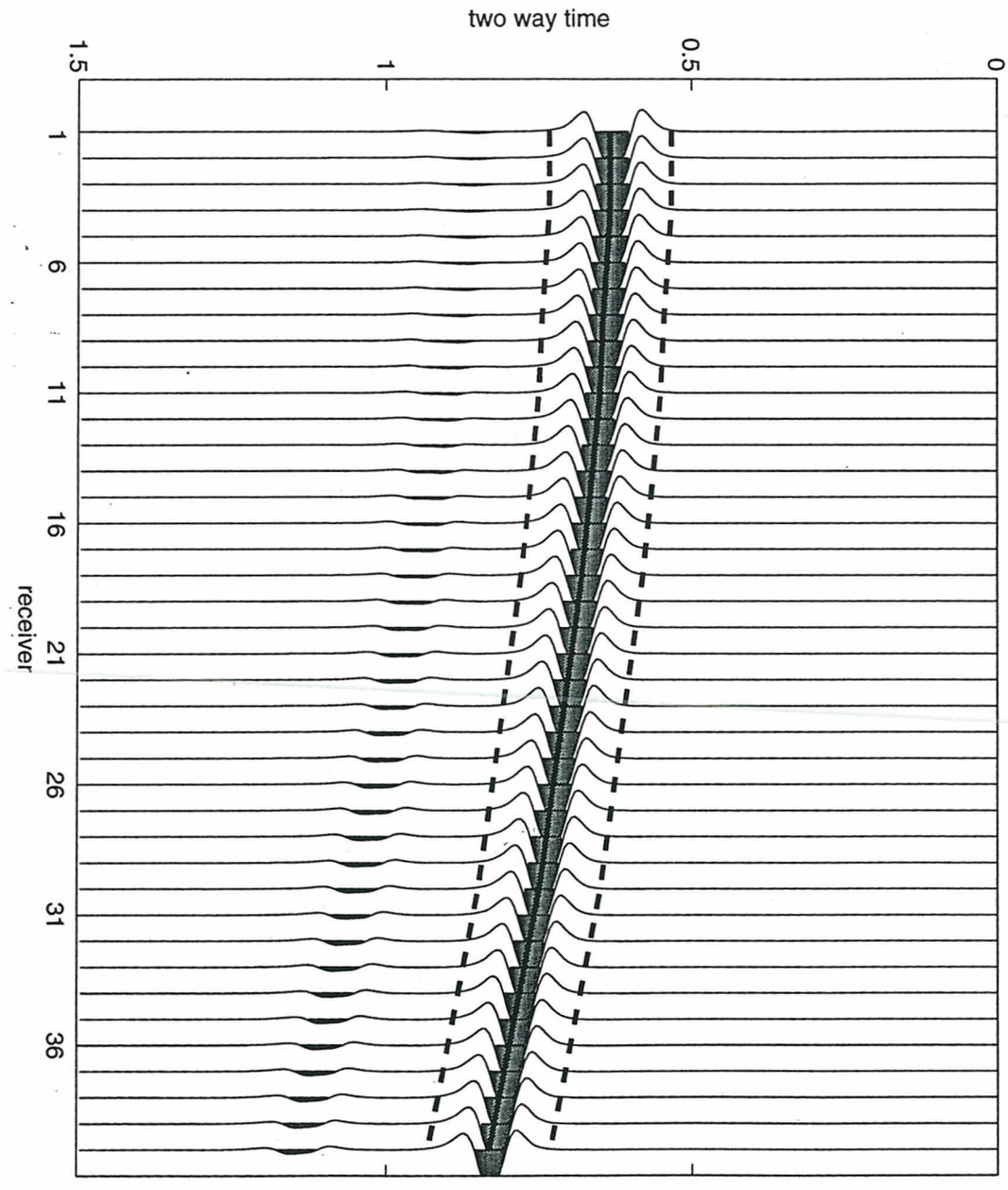

Figure 3: Synthetic data to illustrate the windowing process. See text for detailed description.

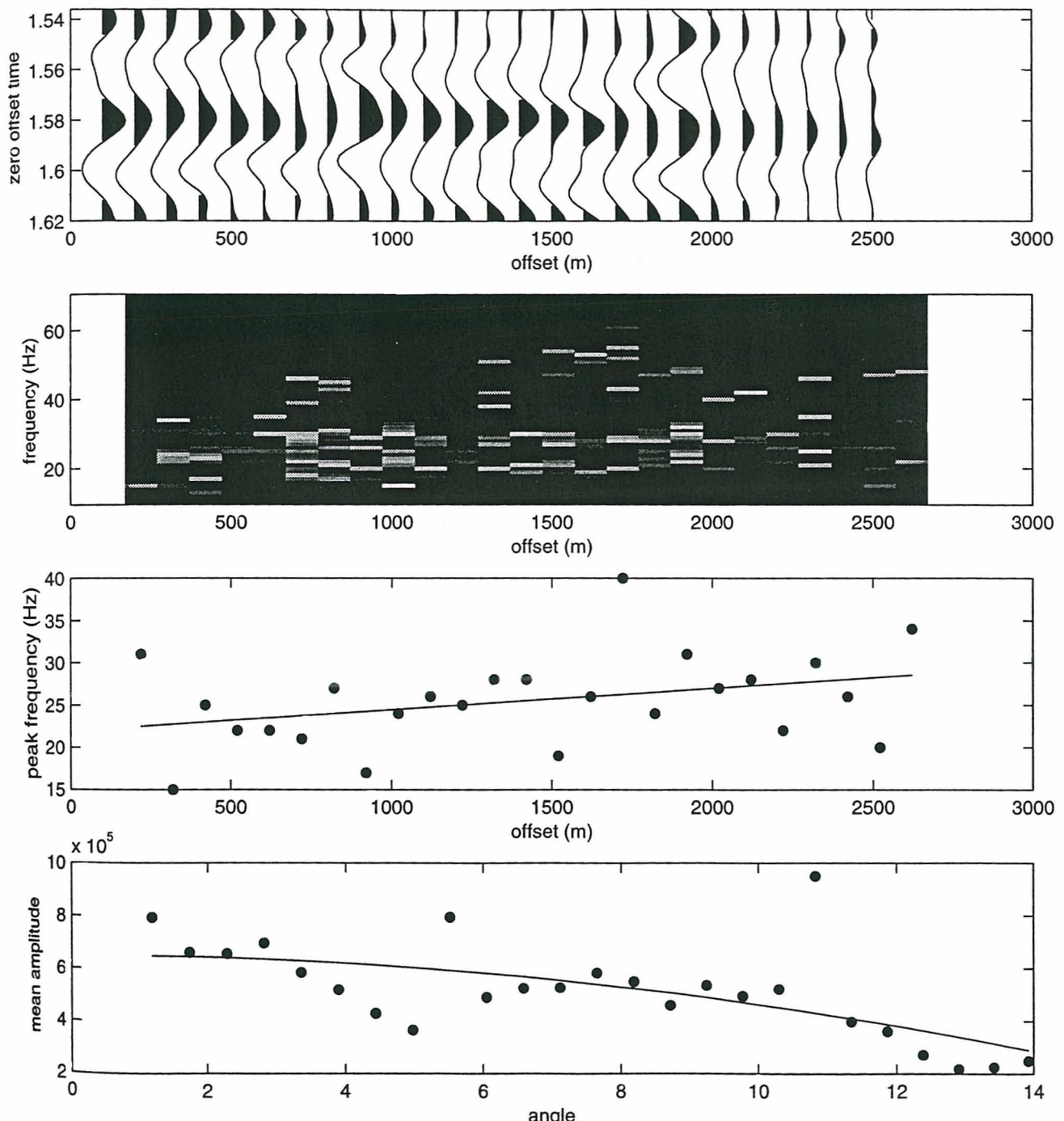

Figure 4: Offset dependent frequency and amplitude calculation for synthetic data shown in Figure 3. The top plot shows the traces chosen by the windowing. The second plot is the power spectrum where lighter means more power. The third plot shows the peak frequency, and the bottom plot shows the amplitude versus incidence angle.

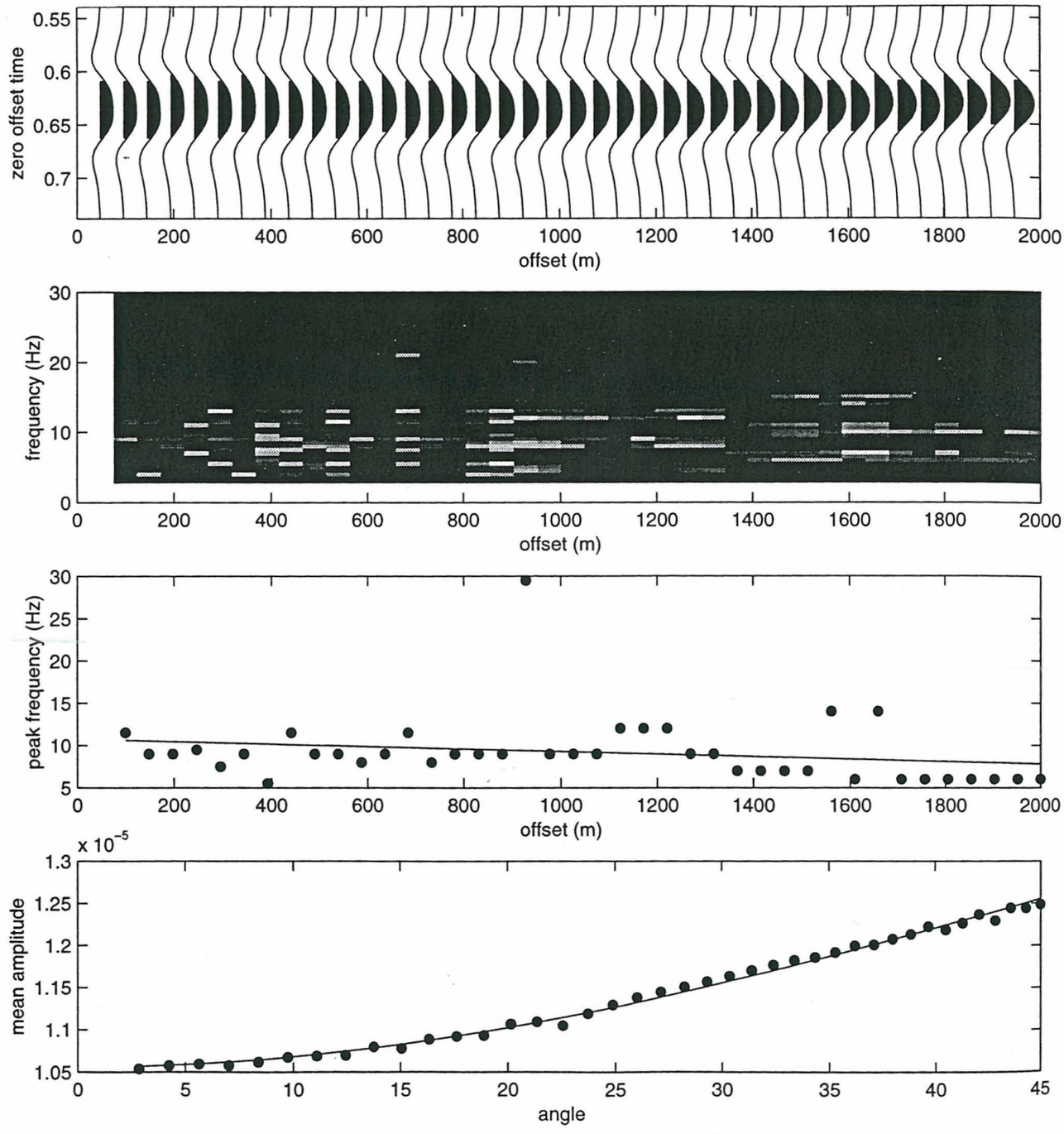

Figure 5: Frequency and amplitude analysis results for horizon 3 at CDP 315. See Figure 4 caption for subplot description.

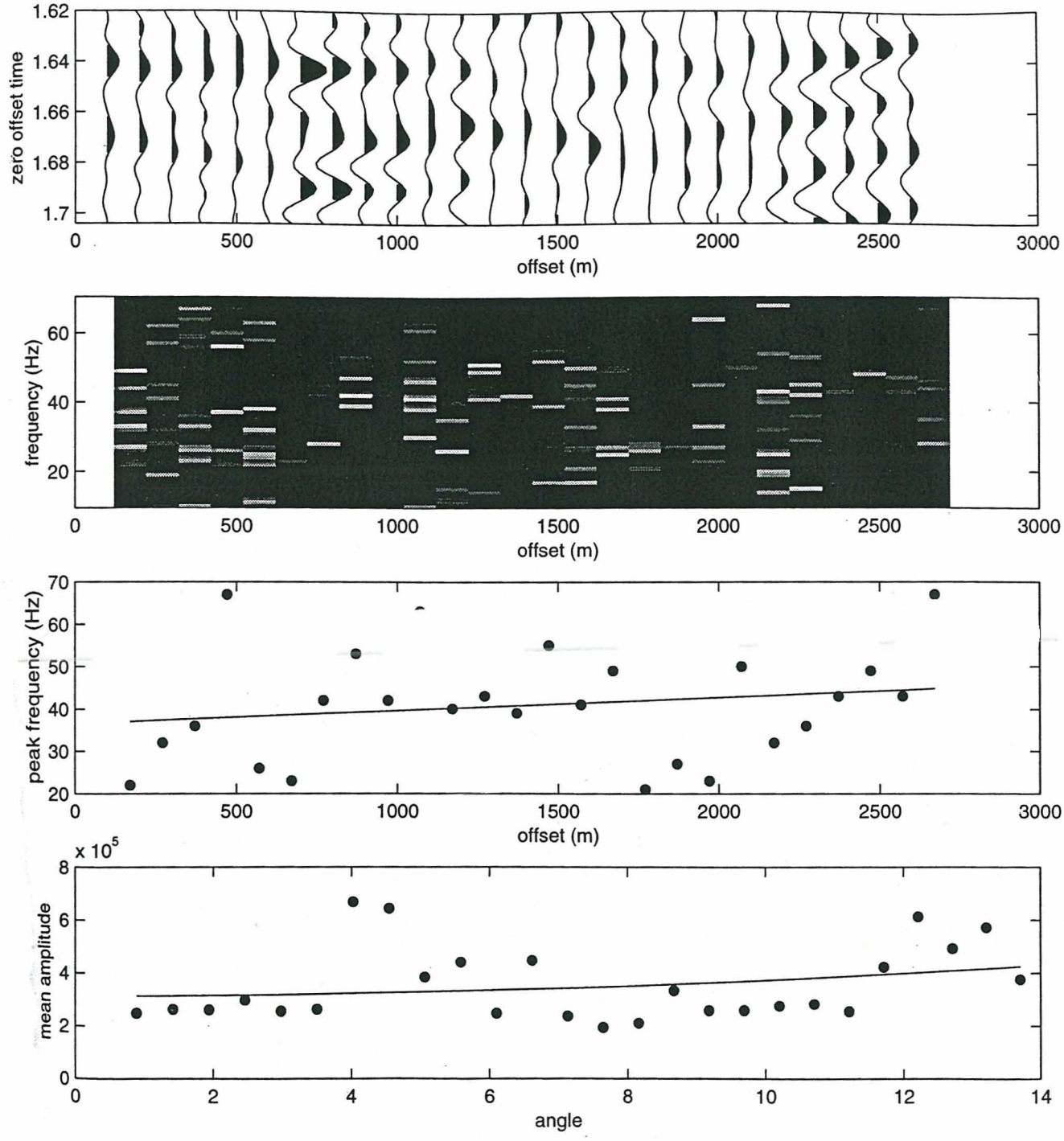

Figure 6: Frequency and amplitude analysis results for horizon 3 at CDP 425. See Figure 4 caption for subplot description.

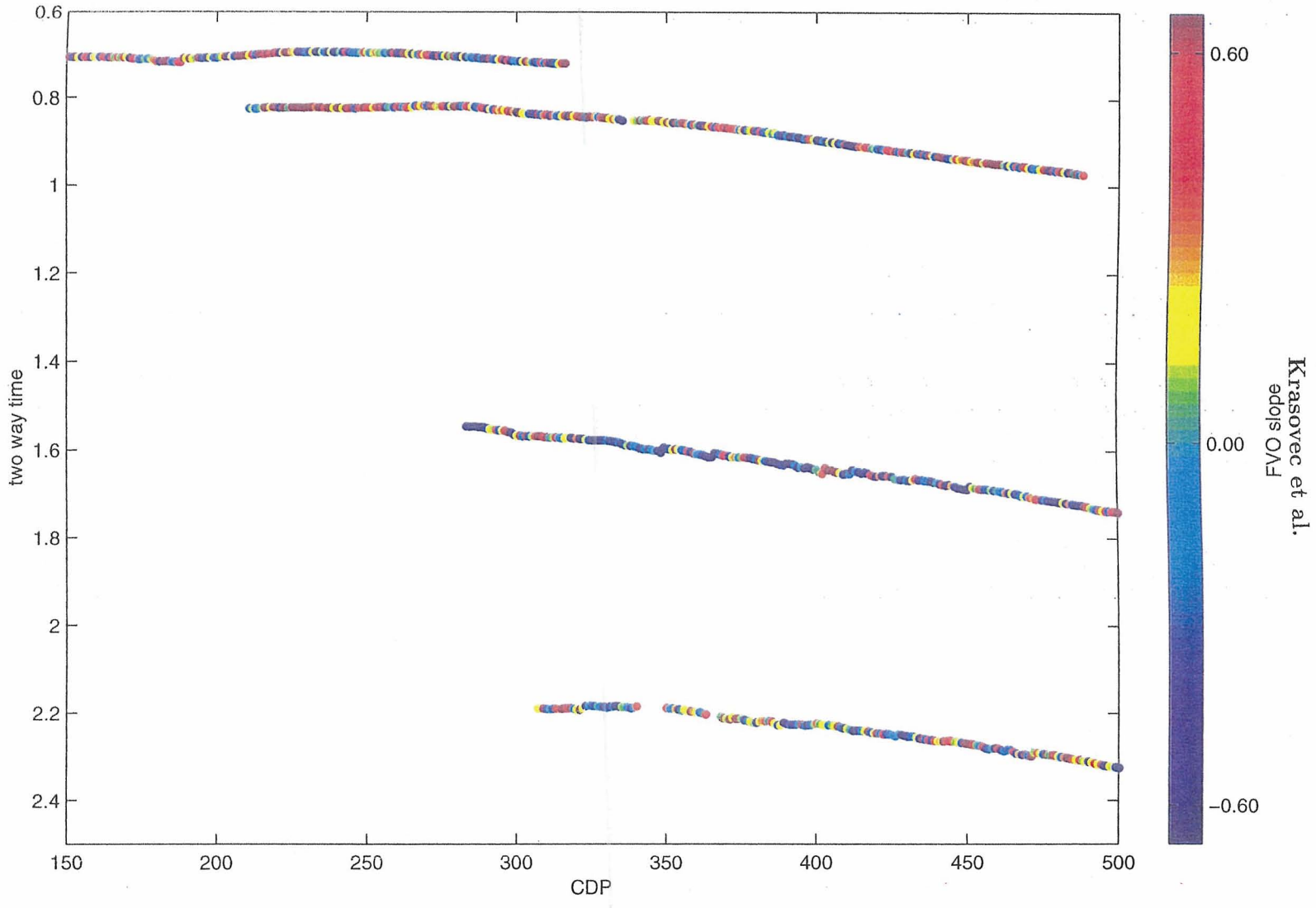

Figure 7: The FVO slope for all four horizons.

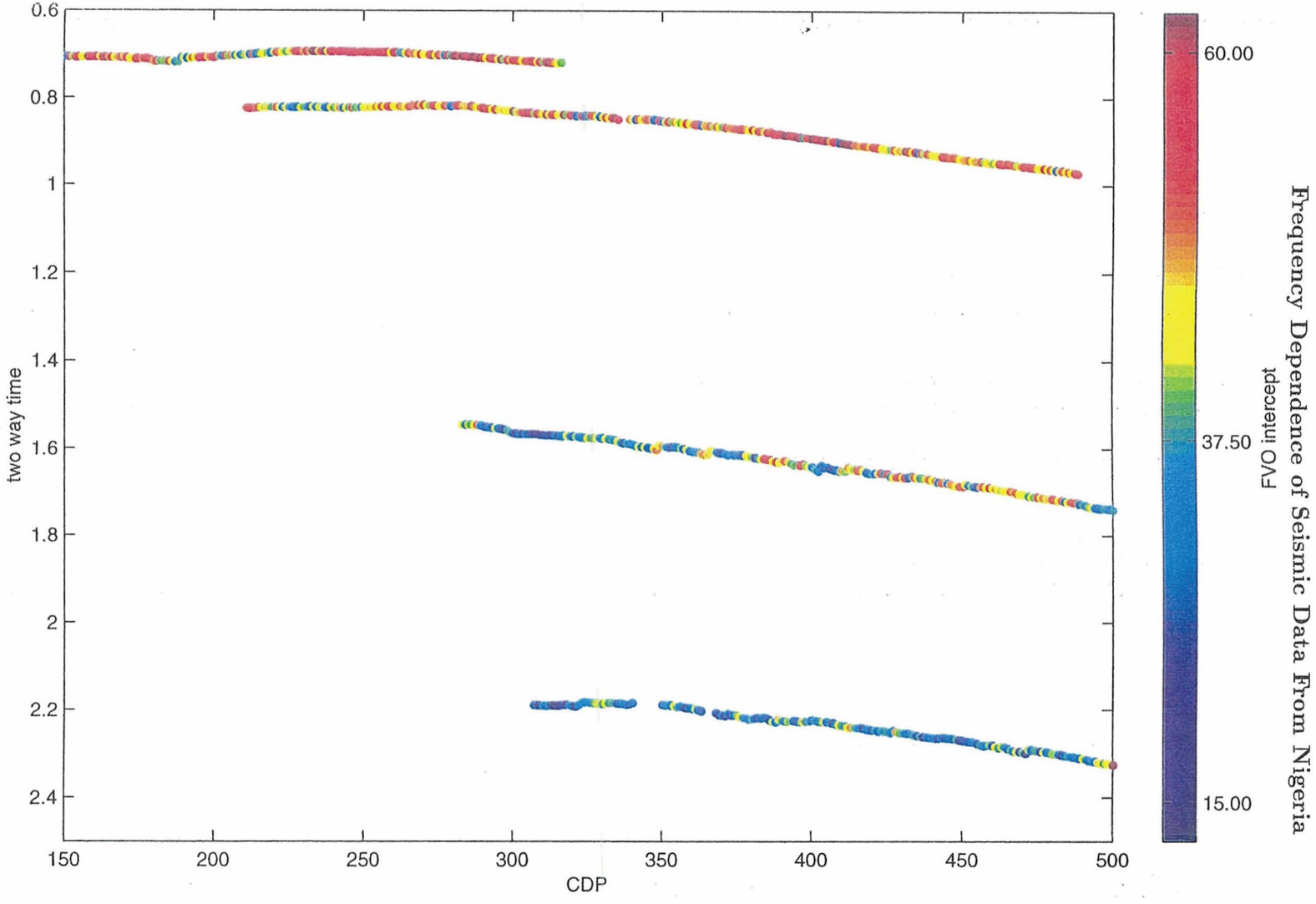

Figure 8: The FVO intercept for all four horizons.

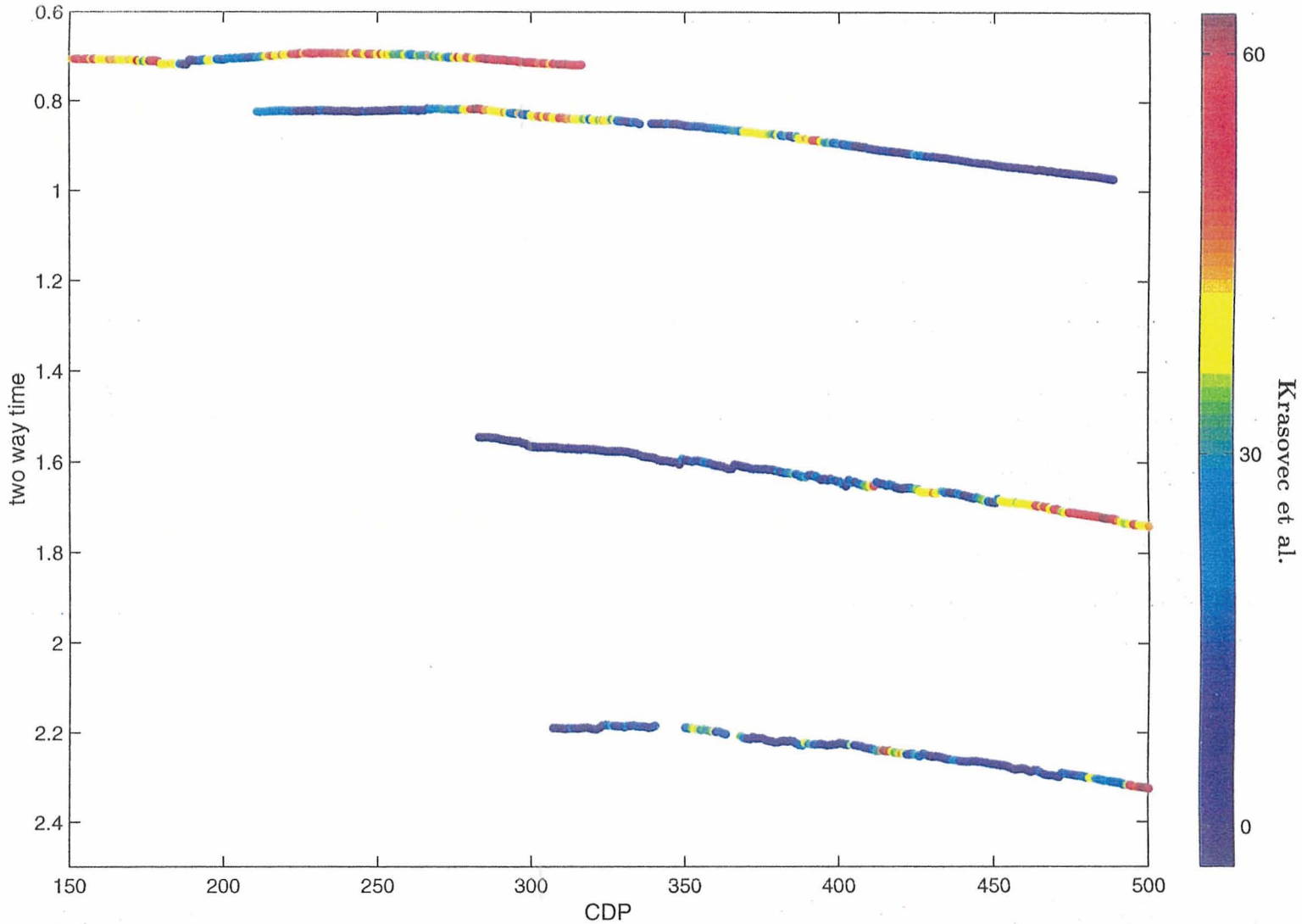

Figure 9: The instantaneous frequency for all four horizons, calculated from the deconvolved poststack data.